Journal of Alloys and Compounds 672 (2016) 397–402

Contents lists available at ScienceDirect

Journal of Alloys and Compounds

journal homepage: http://www.elsevier.com/locate/jalcom

Record-low sintering-temperature (600 °C) of solid-oxide fuel cell electrolyte

Hari Prasad Dasari [a, b, *], Kiyong Ahn [a, 1], Sun-Young Park [a], Jongsup Hong [a], Hyoungchul Kim [a], Kyung Joong Yoon [a], Ji-Won Son [a], Byung-Kook Kim [a], Hae-Weon Lee [a], Jong-Ho Lee [a, **]

[a] High-Temperature Energy Materials Research Center, Korea Institute of Science and Technology, Seoul 136-791, Republic of Korea
[b] Chemical Engineering Department, National Institute of Technology Karnataka, Mangalore 575025, Karnataka, India

ARTICLE INFO

Article history:
Received 25 November 2015
Accepted 20 February 2016
Available online 24 February 2016

Keywords:
Ceramics
Fuel cells
Ceria
Electrolyte
Sintering
Nano-particles

ABSTRACT

One of the major problems arising with Solid-Oxide Fuel Cell (SOFC) electrolyte is conventional sintering which requires a very high temperature (>1300 °C) to fully densify the electrolyte material. In the present study, the sintering temperature of SOFC electrolyte is drastically decreased down to 600 °C. Combinational effects of particle size reduction, liquid-phase sintering mechanism and microwave sintering resulted in achieving full density in such a record-low sintering temperature. Gadolinium doped Ceria (GDC) nano-particles are synthesized by co-precipitation method, Lithium (Li), as an additional dopant, is used as liquid-phase sintering aid. Microwave sintering of this electrolyte material resulted in decreasing the sintering temperature to 600 °C. Micrographs obtained from Scanning/Transmission Electron Microscopy (SEM/TEM) clearly pointed a drastic growth in grain-size of Li-GDC sample (~150 nm) than compared to GDC sample (<30 nm) showing the significance of Li addition. The sintered Li-GDC samples displayed an ionic conductivity of ~1.00×10^{-2} S cm^{-1} at 600 °C in air and from the conductivity plots the activation energy is found to be 0.53 eV.

1. Introduction

Solid-Oxide Cells (SOCs), as fuel and electrolysis cells, shows good conversion efficiency of chemical fuels into electrical energy and hydrogen production by steam electrolysis, respectively [1–3]. Densification of the electrolyte material at lower sintering temperatures still remains as one of the major technical challenges which can save energy and reduce the fabrication costs of SOCs. In recent years, the CeO_2-based materials doped with metal oxides or molten salts decreased the sintering temperature to less than 1000 °C by forming a liquid-phase during sintering step [4–7] but still there is much scope to far reduce the sintering temperature by controlling the nano-particle size, choosing proper liquid-phase additive and heat-treatment methods. Firstly, the sintering driving force can be enhanced by synthesizing the particles in the nano-meter range [8–12]. For nano-particles, the primary mode of densification occurs via grain-boundary diffusion [13]. Thus, the densification behavior and the overall sinterability is determined by the synthesis methods from which nano-particles can be obtained [14–17]. Secondly, sintering effects can also be effected by the addition of sintering aids [4,6,18,19]. Even though, electrolyte materials were successfully synthesized by various techniques, nearly full dense ceria ceramics have been fabricated at a high temperature of 1150–1300 °C [20,21]. Here, we report record-low sintering temperature (600 °C) of gadolinium doped ceria (GDC, $Ce_{0.9}Gd_{0.1}O_{2-\delta}$) electrolyte material by liquid-phase sintering with lithium salt ($LiNO_3$) as an additive and by microwave heat treatments.

When compared to Yttria-Stabilized-Zirconia (YSZ) (state-of-art electrolyte for SOFCs), GDC received a great attention because of its superior ionic conductivity [22,23]. One of the critical challenges that the SOFC electrolytes have is their poor densification behavior and to obtain the full densification, the sintering temperature of the electrolyte has to be raised upto 1500 °C depending on the material

* Corresponding author. Chemical Engineering Department, National Institute of Technology Karnataka, Surathkal, Mangalore 575025, Karnataka, India.
** Corresponding author.
E-mail addresses: energyhari@nitk.edu.in (H.P. Dasari), jongho@kist.re.kr (J.-H. Lee).
[1] Present address: SDI R&D Center, Samsung SDI, 130 Samsung-ro, Suwan, Gyunggi-443803, Republic of Korea.

http://dx.doi.org/10.1016/j.jallcom.2016.02.184
0925-8388/

system [8,9]. The advantage of decreasing the sintering temperature of electrolytes is that the electrolyte can be co-fired with the electrodes without changing their microstructures much at relatively low temperatures [24–26]. Enhanced densification kinetics and overall sinterability of the electrolyte at lower sintering temperature can be achieved by controlling the nano-particle size and adding suitable sintering aids [27]. Most of the studies, however, decreased the sintering temperature down to 950 °C or to 800 °C by either controlling the particle size or choosing suitable sintering aids, respectively, but not choosing the both [4,5,10,11,20,21,27]. In this report, record-low sintering temperature (600 °C) of GDC electrolyte was achieved by controlling the nano-particle size, by adding lithium nitrate salt as a sintering aid and more importantly using microwave energy to enhance the densification kinetics.

2. Experimental

2.1. Synthesis

2.1.1. Synthesis of $Ce_{0.9}Gd_{0.1}O_{2-\delta}$ (nano-GDC)

Co-precipitation method is used to prepare nano-crystalline GDC (nano-GDC) powders [10]. In synthesis procedure, anhydrous ethyl alcohol is used as a solvent medium instead water. The precipitates were washed with ethanol to remove the impurities. In order to obtain nano-GDC, the precipitates were oven dried at 80 °C in air for 48 h.

2.1.2. Synthesis of lithium doped GDC (nano-Li-GDC)

Lithium nitrate (Sigma–Aldrich Chemicals) addition as a sintering aid for the obtained nano-GDC powders was investigated by dissolving 5 mol% of Li salt in ethanol and the nano-GDC powder was added in order to form a suspension. Evaporation of the salt was carried at 70 °C and the resulting product was dried over night at 80 °C.

2.1.3. Micro-GDC and micro-Li-GDC samples

The Micro-GDC is the commercial GDC powder obtained from Rhodia. Micro-Li-GDC samples were obtained in the similar procedure to that of nano-Li-GDC samples.

2.2. Microwave sintering

For observing the sintering tendency and electrical conductivity, the powders were heat-treated (150 °C for 2 h) and pellets were obtained by uni-axial pressing (50Mpa) and by cold isostatic pressing (150Mpa). The pressed pellets were sintered using a microwave furnace (UMF-04, Unicera) at 550 °C and 600 °C for 1 h. Heating rate and cooling rate was maintained at 20 °C/min. In conventional sintering, pellets were heated up to desired temperature and cooled down to room temperature after the specific holding time. The heating rate and cooling rate was 5 °C/min. The conductivity measurements were obtained in the temperature range of 400–600 °C in air. The physical characterization of the samples were carried out as described in our earlier report [10].

3. Results and discussion

In order to achieve such a low sintering temperature for densification by liquid-phase sintering, the control of nano-particle size is very important because it determines the surface curvature, contact stress, and capillary effects, thereby easing the densification. For isothermal sintering, the normalized densification rate $d\rho/\rho dt$ according to the literature [5] may be written as:

$$d\rho/\rho dt = F(\rho,T)C(G)\left(\delta D/G^3\right) \quad (1)$$

where $C(G)$ and $(\delta D/G^3)$ is normalized driving force and kinetic factor for the grain size G, respectively. And δ and D is the grain boundary thickness and grain boundary diffusion coefficient, respectively. $F(\rho,T)$ may depend on density and pore size distribution, and possibly also on temperature and is independent of grain size [28]. The normalized driving force $C(G)$ may be $\gamma_{ss}\,\Omega/GkT$ for grain boundary diffusion or $2\,\gamma_{1v}/r_p$ for capillary pressure in case of liquid phase sintering with interfacial energies of γ_{ss} and γ_{1v}, the atomic volume Ω, and the pore radius r_p. Thus, if the GDC particle size is controlled to nano-size without any hard agglomeration then the r_p value in Equation (1) also becomes very small and the small amounts of liquid-phase result in high hydrostatic pressures with enhanced capillary effects. With small amounts of liquid during liquid-phase sintering, one can follow the classical arguments of Heady and Cahn [29]. The liquid tends to eliminate the solid–vapor interface. During the later stages of sintering the decrease of the liquid–vapor pore surface area will be the driving for the densification. To further enhance the densification process, the concept of microwave-sintering is also introduced along with the liquid-phase sintering. Enhancement in the densification in case of microwave sintering can be due the reverse thermal

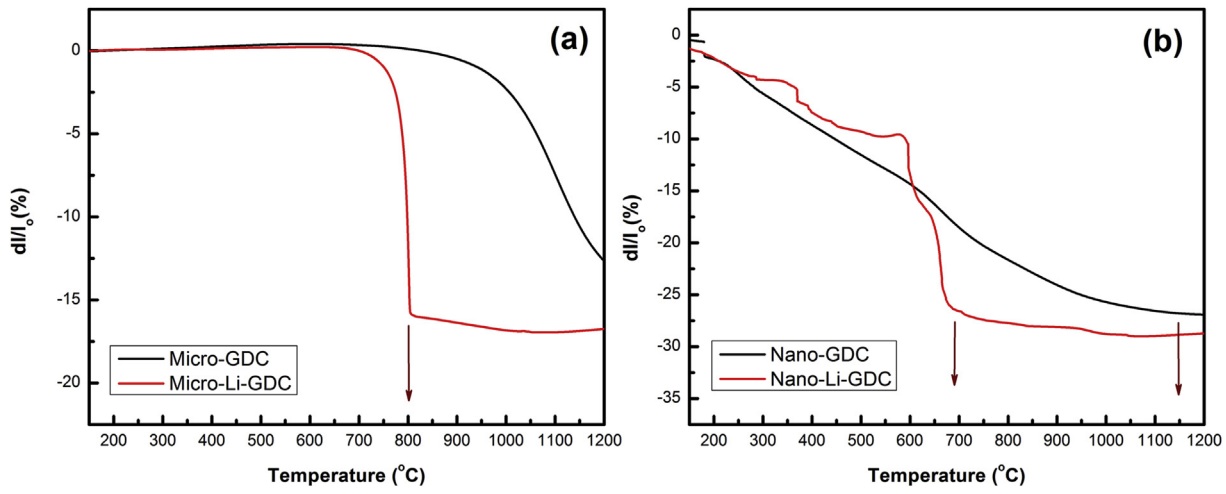

Fig. 1. Linear shrinkage behavior of (a) micro-GDC and micro-Li-GDC (b) nano-GDC and nano-Li-GDC.

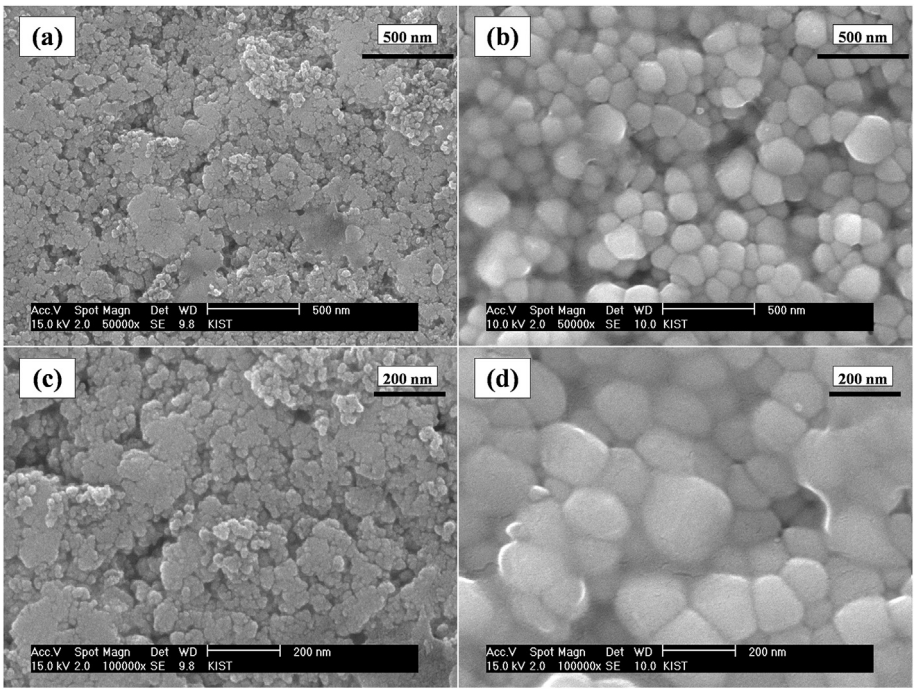

Fig. 2. Scanning electron microscope images of (a & c) nano-GDC and (b & d) nano-Li-GDC pellets microwave sintered at 600 °C for 1 h.

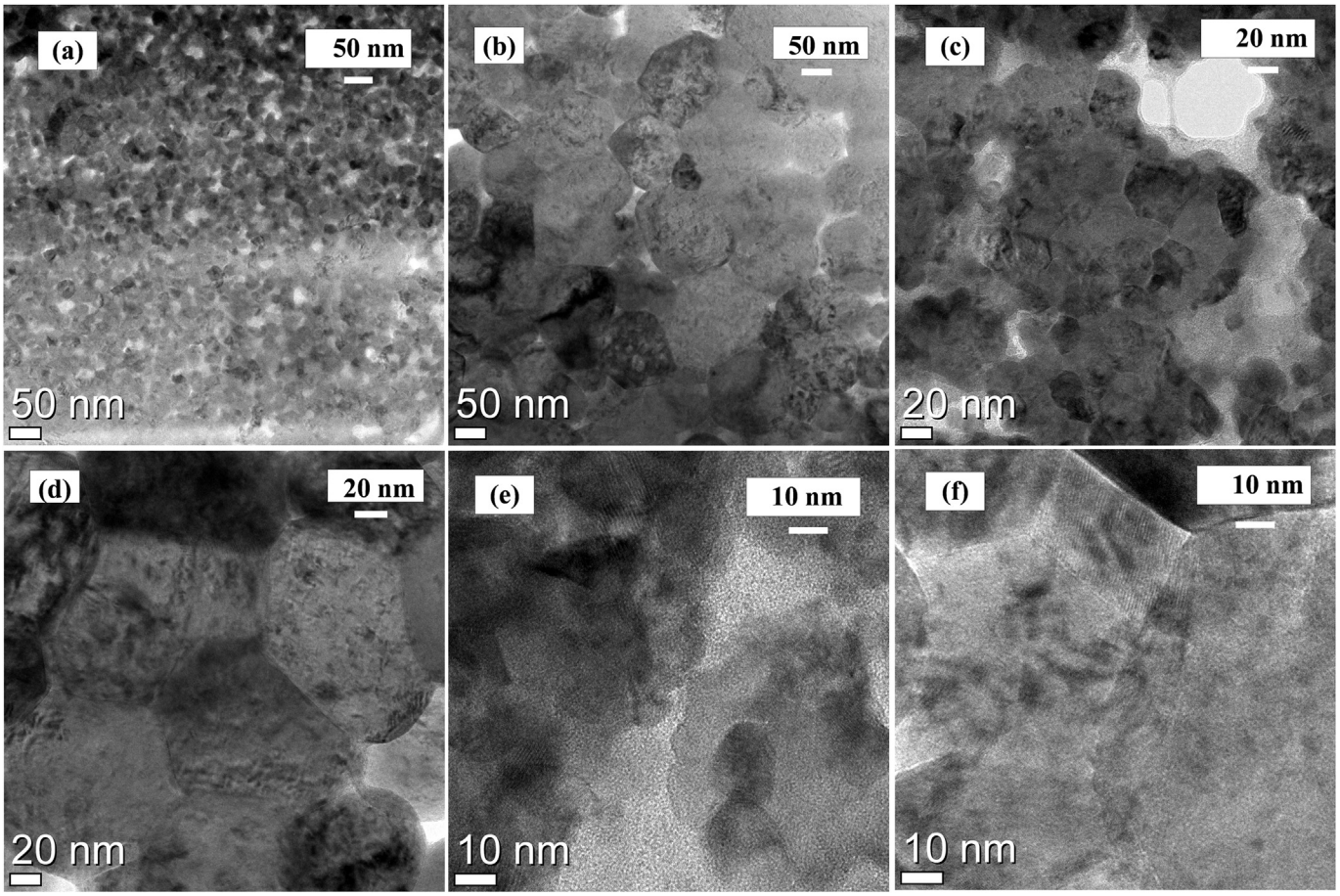

Fig. 3. High-resolution transmission electron microscope images of (a,c,e) nano-GDC pellets and (b,d,f) nano-Li-GDC pellets microwave sintered at 600 °C for 1 h.

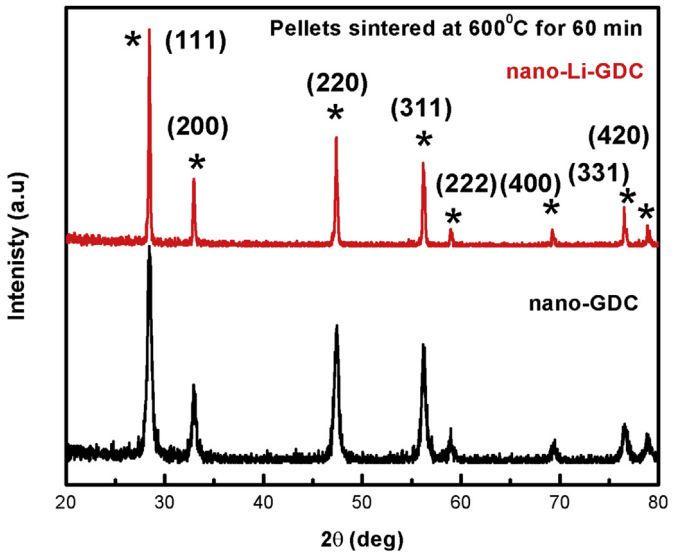

Fig. 4. X-ray diffraction patterns of nano-GDC and nano-Li-GDC pellets microwave sintered at 600 °C for 1 h.

gradient phenomenon [30]. This temperature gradient can cause reverse porosity gradient and thus accelerate the densification than compared to conventionally sintered samples [30]. Microwave sintering requires less thermal energy to start the sintering process than compared to its counterpart [30]. Thus, the combination of the three factors *i.e.* nano-particle size-effect, liquid-phase and microwave sintering effects can play a critical role in obtaining full-dense bodies at a critically low sintering temperature.

Nano-particle size can show a positive effect on sintering only if one can minimize the hard agglomeration of the nano-particles which usually occurs by neck connection during the synthesis [31]. From Supplementary Fig. S1, it is manifested that the nano-GDC obtained by co-precipitation method using ethanol as a solvent resulted in both smaller agglomerate and nano-particle sizes than compared to its counterpart prepared by same method but using water as a solvent. HR-TEM images, XRD, EDS microanalysis and Raman spectroscopy analyses confirms the presence of nano-crystalline particles, formation of solid-solution and the stoichiometry of the GDC phase (See Figs. S2, S3, S4 and Table S1 in Supporting Information).

In the next step, the effect of nano-particle size and lithium-doping on the linear shrinkage spectra were investigated in a conventional dilatometer instrument and the results were depicted in Fig. 1. Unlike the earlier reports [5,14,32], where a high isostatic pressure is applied (during preparation of green compact pellets) in the process of achieving fully dense bodies at low-sintering temperature, in the present investigation the green compact pellets were obtained by CIP at only 150Mpa. Firstly, from Fig. 1, it can be clearly noticed that the micro-GDC and nano-GDC samples have different shrinkage behaviors and the later one showed enhanced sinterability due to its size effect. Secondly, the micro-Li-GDC and nano-Li-GDC samples showed different linear shrinkage behavior than their counterparts. Nano-Li-GDC showed maximum linear shrinkage and at much low temperature than micro-Li-GDC sample. Fig. 1 further confirms the classical arguments of Heady and Cahn [29] for liquid-phase sintering which was described earlier. As the nano-GDC is very small, r_p in Equation (1) also becomes very small and already small amount of liquid (5 mol% of Lithium nitrate) result in high hydrostatic pressures. The micro-GDC sample did not show such rapid densification at these low temperature (<700 °C). From Fig. 1b the nano-GDC sample showed a broad sintering range up to 1000 °C as common for co-precipitation method [10]. It can also be seen that the linear shrinkage (ΔL/L (%)) increased significantly (26%) for nano-Li-GDC sample below 700 °C, indicating that the full densification can be achieved below 700 °C. For micro-Li-GDC sample, the maximum linear shrinkage (17%) was noticed in a shorter temperature range of 110 °C (from 575 °C to 685 °C). Addition of Li content to GDC system leads to the substitution of Ce^{4+} (coordinate number of 8, 0.97 Å) or Gd^{3+} (coordinate number of 8, 1.053 Å) by Li^{+} (coordinate number of 8, 0.92 Å) as shown in the following reactions [7]:

$$Li_2O \rightarrow 2Li'''_{Ce} + 3V_o^{\cdot\cdot} + O_o^X \text{ (for } CeO_2) \quad (2)$$

$$Li_2O \rightarrow 2Li'''_{Gd} + 2V_o^{\cdot\cdot} + O_o^X \text{ (for } Gd_2O_3) \quad (3)$$

The doping of Li in both Gd and Ce sites is possible [33]. From equation (2) and equation (3) it can be clearly seen that Li doping enhances the vacancy concentration and thus enhances the flow of the atoms alongside the grain boundary which can significantly lower the sintering temperature [4]. Undersized dopants results lattice distortion which in turn provides the grain boundary mobility [34]. In order to find out the sintering temperature at which full density of Li-GDC can be obtained, the green pellets were heat-treated at 550 and 600 °C for 1 h in microwave furnace. Table S2 shows the relative density of nano-GDC and nano-Li-GDC pellets heat treated at various temperatures by conventional sintering and by microwave sintering. The conventional sintering carried out at 800 °C/3 h showed a relative density of ~80 and ~85% for nano-GDC and nano-Li-GDC samples whereas the samples

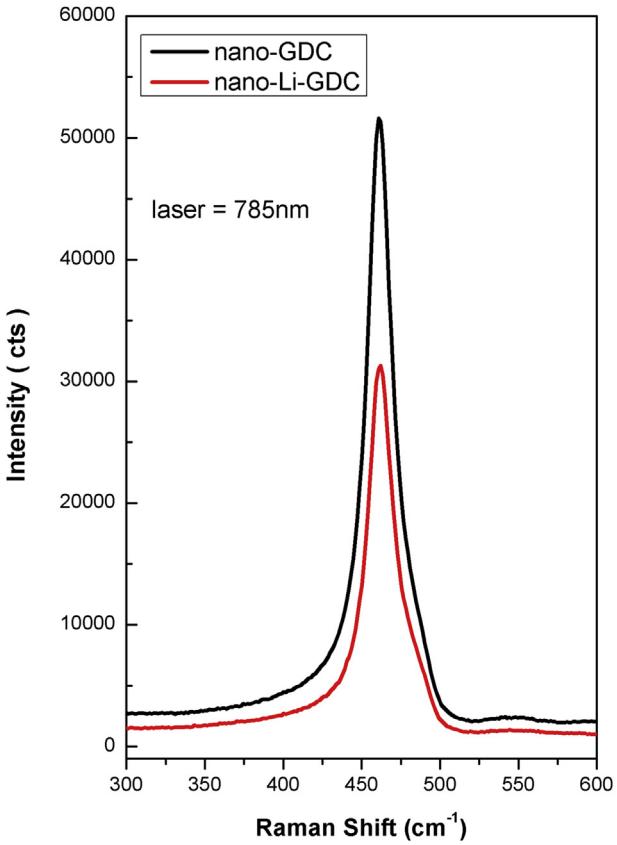

Fig. 5. Raman spectra of nano-GDC and nano-Li-GDC pellets microwave sintered at 600 °C for 1 h.

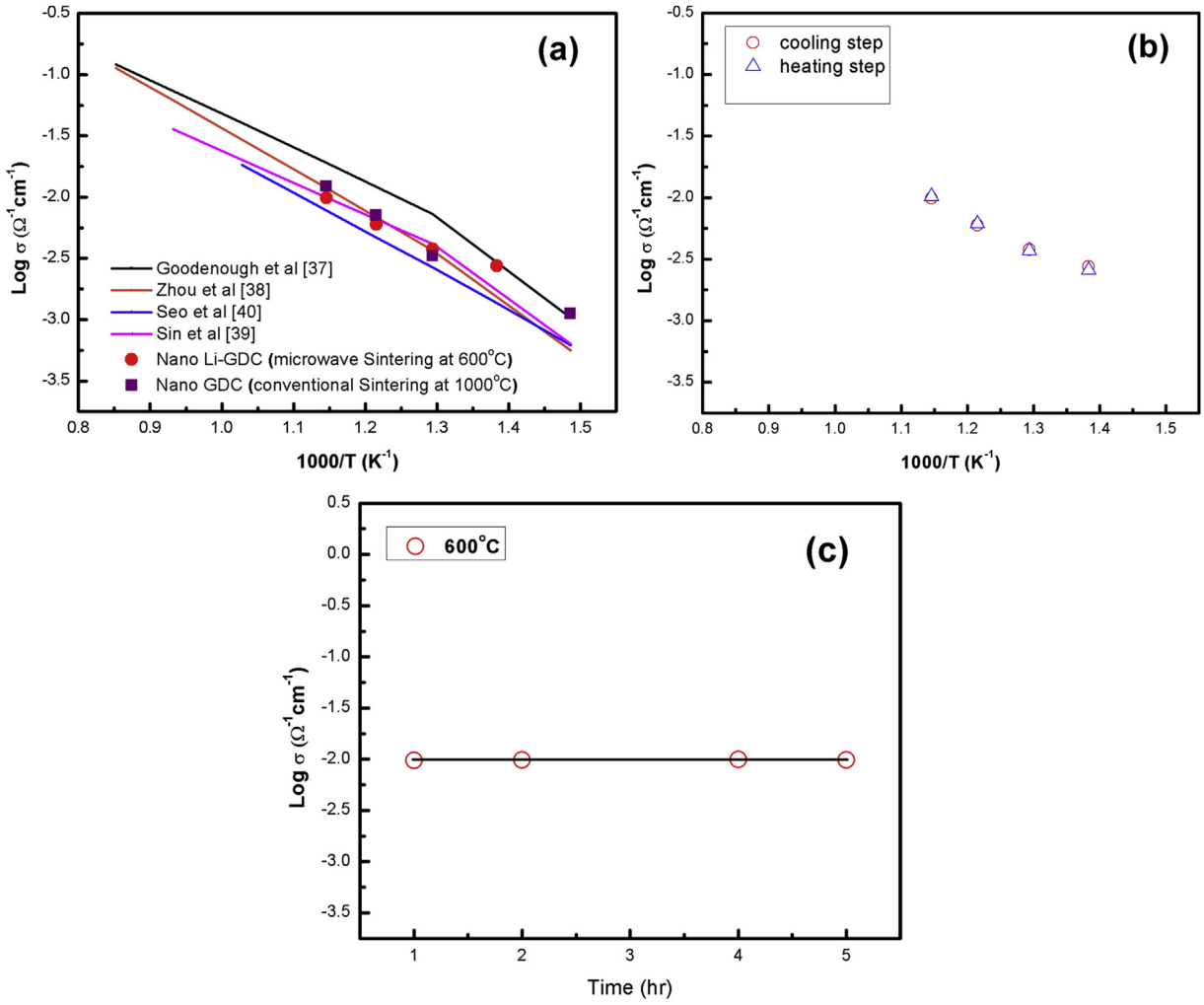

Fig. 6. Electrical conductivity data of nano-GDC and nano-Li-GDC pellets sintered at 600 °C for 1 h (a) Arrhenius plot (b) during cooling and heating steps (c) conductivity plot of nano-Li-GDC operated at 600 °C for 5 h.

displayed a relative density of ~74% and ~98% at a microwave sintering temperature of 600 °C/1 h. This clearly shows the significance of liquid-phase sintering and microwave sintering effect on prepared samples.

Fig. 2 depicts SEM micrograph of nano-GDC and nano-Li-GDC pellets that are microwave-sintered at 600 °C for 1 h. As shown in Fig. 2, nano-GDC pellet (Fig. 2a and c) have many pores whereas a dense microstructure was observed for nano-Li-GDC pellet (Fig. 2b and d) which is in accordance with the density measured from the Archimedes method. It is also clearly evidenced from the SEM micrographs that a drastic increase in grain size was observed for nano-Li-GDC pellet than compared to its counterpart. This further supports the linear shrinkage data (Fig. 1) and gives evidence that the process of sintering phenomena in nano-Li-GDC pellet is different and demonstrates an enhanced sintering activity for this sample than compared to nano-GDC pellet. These results indicate that the nano-particle size, Li doping and microwave heat treatment enhances the rate of densification drastically and promote mobility in the grain boundary. In order to gain further knowledge to the grain-size and grain-boundaries HR-TEM analysis is carried on these samples.

Fig. 3 illustrates the grain-morphology of the microwave-sintered pellets (600 °C for 1 h) at high magnification using HR-TEM images. Fig. 3a clearly evidences that the nano-GDC showed not enough densification with many pores and particles necking each other even though it showed some densification in certain areas. The grain-size was below 50 nm. Fig. 3b unambiguously, showed highly packed grains with clear grain boundaries. Even though a very low sintering temperature (600 °C) is used for the heat-treatment, the grains appeared spherical and relaxed. The grain-size was below 150 nm. No secondary phases were detected at the grain boundary regions. Generally, presence of a molten phase on the surface of the pellet results in poor mechanical properties of the pellets [20] and no such phases were observed on the surface of nano-Li-GDC pellets (Fig. 3c). Fig. 3f clearly shows that the nano-Li-GDC grain and grain-boundaries are clean without any amorphous oxide grain boundary layer indicating that the Li dopant completely diffuses into the GDC grains. Ceria based materials show good solubility limit for many dopants [4,32,35]. The Li^{+} ions are dissolving in Ce/Gd lattice during the final stage of sintering. Due to this, in the present study ion-blocking grain boundary layer and significant increase in the electronic conductivity is not observed (conductivity results are depicted in Fig. 6).

Fig. 4 illustrates the XRD patterns of the nano-GDC and nano-Li-GDC pellets sintered at 600 °C for 1 h. In these samples only cubic fluorite phase is detected. No additional reflections, from the presence of the extra phases (impurities) in the samples, could be revealed. The crystallite sizes of nano-GDC and nano-Li-GDC pellets

were ~27 nm and ~75 nm, respectively and corroborates with TEM images of the corresponding samples. Lattice parameters of nano-GDC and nano-Li-GDC pellets were ~5.428 Å and ~5.431 Å. It should be noted that a lattice expansion in nano-Li-GDC sample is observed. This indicates that the Li^+ ions help in segregation of Gd^{3+} ions back into the sample [32]. Formation of liquid-phase enhances the atomic mobility and gradient in chemical potential at the same time, if dopant substitution also takes place than the oxygen vacancy concentration also enhances [4]. Fig. 5 shows the Raman spectra of these samples, and the peak intensity has been decreased significantly with the addition of the Li^+ ions in the ceria lattice. This signifies a lattice deformation with the addition of Li^+ ions. Such kind of deformation may enhance the oxygen mobility [36]. All these factors results in total enhancement of the flux of atoms along the grain boundary region which can enhance the sintering density at much lower temperatures. This clearly demonstrates that a good combination of nano-particle size, liquid additive and microwave heat-treatment can drastically reduce the sintering temperature for full densification.

Arrhenius plot for the conductivity of nano-GDC (conventional sintered at 1000 °C) and nano-Li-GDC (microwave sintered at 600 °C) pellets is depicted in Fig. 6a and the results were comparable with the literature data [37–40]. The nano-Li-GDC sample exhibited a conductivity of ~1.00×10^{-2} Scm^{-1} at 600 °C. The activation energy of this sample was calculated from the conductivity plots (Supplementary Fig. S5) and was found to be 0.53 eV. In Fig. 6b, the conductivity of the nano-Li-GDC sample during cooling and heating steps were identical indicating that the formation of the insulating phase is not observed in this sample which was as expected from the results of TEM observations. Fig. 6c, shows the conductivity of the nano-Li-GDC sample at 600 °C operated for 5 h where we can clearly notice that there were no changes in the conductivity results indicating that there were no microstructural changes in the sample.

4. Conclusions

In conclusion, the sintering temperature of SOFC electrolyte is drastically decreased down to 600 °C due to the combinational effects of particle size reduction, liquid-phase sintering mechanism and microwave sintering. Dilatometry studies demonstrated that the nano-particle size reduction and Lithium doping has a positive effect sintering the samples at much lower temperatures. Nano-Li-GDC sample showed a maximum linear shrinkage of 26% below 700 °C. SEM and TEM micrographs of microwave sintered nano-GDC and nano-Li-GDC samples pointed the significance of Li addition as dopant and its role in liquid. With the addition of Li to GDC sample, the grain growth is ~6 times larger than the GDC sample. The conductivity data obtained for the sintered samples is much similar to the literature data and this confirms that the addition of Li has not showed any adverse effects. The ionic conductivity of nano Li-GDC is ~1.00×10^{-2} S cm^{-1} at 600 °C in air and from the conductivity plots the activation energy is found to be 0.53 eV. A good combination of nano-particle size, liquid-additive and microwave heat-treatment can drastically reduce the electrolyte sintering temperature.

Acknowledgments

This work was supported by the New & Renewable Energy Core Technology Program of the Korea Institute of Energy Technology Evaluation and Planning (KETEP) granted financial resource from the Ministry of Trade, Industry & Energy, Republic of Korea (No. 20143030031430) and partially funded by the Institutional Research Program (IRP) of KIST (No. 2E26081). This work is conducted at KIST.

Appendix A. Supplementary data

Supplementary data related to this article can be found at http://dx.doi.org/10.1016/j.jallcom.2016.02.184.

References

[1] S. Tao, J.T.S. Irvine, Nat. Mater 2 (2003) 320–323.
[2] E.D. Wachsman, K.T. Lee, Science 334 (2011) 935–939.
[3] A. Brisse, J. Schefold, M. Zahid, Int. J. Hydrogen Energy 33 (2008) 5375–5382.
[4] J. Nicholas, L. Dejonghe, Solid State Ionics 178 (2007) 1187–1194.
[5] C. Kleinlogel, L.J. Gauckler, Adv. Mater 13 (2001) 1081–1085.
[6] D. Hari Prasad, S.Y. Park, H. Ji, H.-R. Kim, J.-W. Son, B.-K. Kim, et al., Ceram. Int. 38 (2012) S497–S500.
[7] T. Zhu, Y. Lin, Z. Yang, D. Su, S. Ma, M. Han, et al., J. Power Sources 261 (2014) 255–263.
[8] P.-L. Chen, I.-W. Chen, J. Am. Ceram. Soc. 80 (1997) 637–645.
[9] J.-G. Li, T. Ikegami, Y. Wang, T. Mori, J. Am. Ceram. Soc. 85 (2002) 2376–2378.
[10] D. Hari Prasad, H.-R. Kim, J.-S. Park, J.-W. Son, B.-K. Kim, H.-W. Lee, et al., J. Alloys Compd. 495 (2010) 238–241.
[11] D.H. Prasad, J.-W. Son, B.-K. Kim, H.-W. Lee, J.-H. Lee, J. Eur. Ceram. Soc. 28 (2008) 3107–3112.
[12] J. Liang, Electrochim. Acta 178 (2015) 321.
[13] C. Herring, J. Appl. Phys. 21 (1950) 301.
[14] C. Kleinlogel, Solid State Ionics 135 (2000) 567.
[15] T. Zhang, P. Hing, H. Huang, J. Kilner, J. Eur. Ceram. Soc. 22 (2002) 27–34.
[16] E. Jud, C.B. Huwiler, L.J. Gauckler, J. Am. Ceram. Soc. 88 (2005) 3013–3019.
[17] J. Luo, R. Stevens, J. Am. Ceram. Soc. 82 (1999) 1922–1924.
[18] E. Jud, L. Gauckler, S. Halim, W. Stark, J. Am. Ceram. Soc. 89 (2006) 2970.
[19] Z. Tianshu, P. Hing, H. Huang, J. Kilner, J. Mater. Sci. 37 (2002) 997.
[20] P.-L. Chen, I.-W. Chen, J. Am. Ceram. Soc. 76 (1993) 1577.
[21] M.N. Rahaman, Y.C. Zhou, J. Eur. Ceram. Soc. 15 (1995) 939.
[22] B.C.H. Steele, J. Mater. Sci. 36 (2001) 1053.
[23] S.M. Haile, Acta Mater 51 (2003) 5981.
[24] C. Jin, Y. Mao, N. Zhang, K. Sun, Int. J. Hydrogen Energy 40 (2015) 8433–8441.
[25] H. Dai, H. Chen, S. He, G. Cai, L. Guo, J. Power Sources 286 (2015) 427–430.
[26] A. Azzolini, J. Downs, V.M. Sglavo, J. Eur. Ceram. Soc. 35 (2015) 2119–2127.
[27] V. Esposito, M. Zunic, E. Traversa, Solid State Ionics 180 (2009) 1069–1075.
[28] I.-W. Chen, X.-H. Wang, Nature 404 (2000) 168.
[29] R. Heady, J. Cahn, Metall. Trans. 1 (1970) 185–189, http://dx.doi.org/10.1007/BF02819260.
[30] R. Chockalingam, S. Chockalingam, V.R.W. Amarakoon, J. Power Sources 196 (2011) 1808.
[31] S. Wang, Y. Zhai, X. Li, Y. Li, K. Wang, J. Am. Ceram. Soc. 89 (2006) 3577.
[32] L. Zhang, R. Lan, P.I. Cowin, S. Tao, Solid State Ionics 203 (2011) 47–51.
[33] Y. Lei, Y. Ito, N.D. Browning, T.J. Mazanec, J. Am. Ceram. Soc. 85 (2002) 2359.
[34] J.-S. Lee, K.-H. Choi, B.-K. Ryu, B.-C. Shin, I.-S. Kim, Mater. Res. Bull. 39 (2004) 2025.
[35] H. Yahiro, T. ohuchi, K. Eguchi, H. Arai, J. Mater. Sci. 23 (1988) 1036.
[36] I. Atribak, A. Buenolopez, A. Garciagarcia, J. Catal. 259 (2008) 123–132.
[37] K. Huang, M. Feng, J.B. Goodenough, J. Am. Ceram. Soc. 81 (1998) 357.
[38] X.-D. Zhou, W. Huebner, I. Kosacki, H.U. Anderson, J. Am. Ceram. Soc. 85 (2002) 1757.
[39] A. Sin, Solid State Ionics 175 (2004) 361.
[40] D.J. Seo, K.O. Ryu, S. Bin Park, K.Y. Kim, R.-H. Song, Mater. Res. Bull. 41 (2006) 359.